Supporting Information

Aldol Condensation of Mixed Oxygenates on TiO_2

Brandon Oliphant, Mathew Rasmussen, Laura Paz Herrera, Mike Griffin, J. Will Medlin*

Department of Chemical and Biological Engineering, University of Colorado Boulder, Boulder, Colorado 80303, USA

*Corresponding author email: Will.Medlin@colorado.edu (J.W. Medlin)

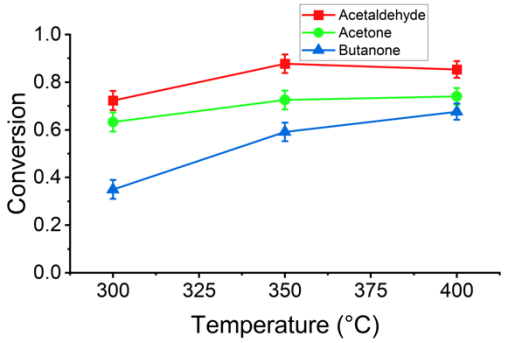

Supplemental Figure 1. High temperature SAC conversion: Conversion plotted as a function of temperature for reactions of acetaldehyde, acetone and butanone over a TiO_2 catalyst. Reactions began at 300 °C and were held at each temperature for 3 hours before ramping to the next temperature over a 15-minute period.

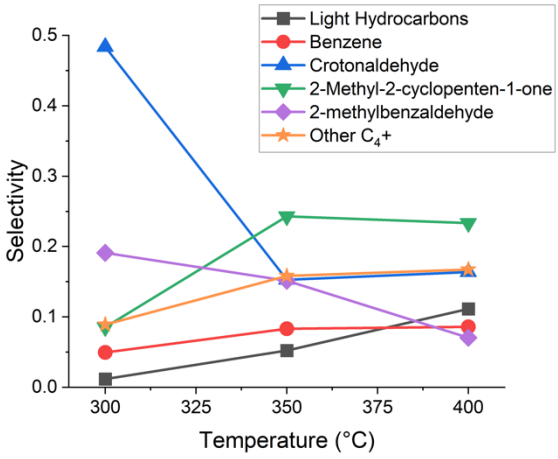

Supplemental Figure 2. High temperature acetaldehyde SAC selectivity: Selectivity and reaction pathways for the SAC of acetaldehyde over a TiO_2 catalyst at 300 °C, 350 °C, 400 °C.

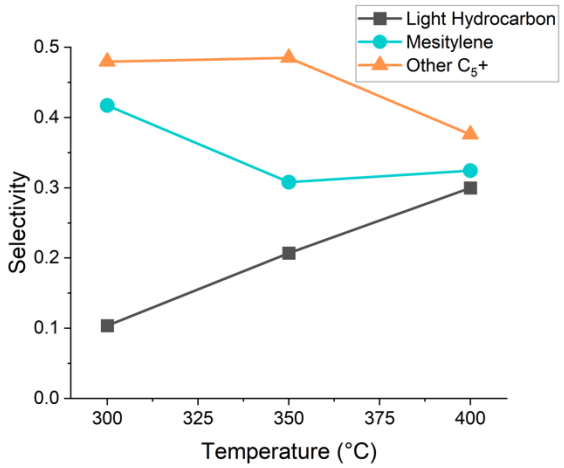

Supplemental Figure 3. High temperature acetone SAC selectivity: Selectivity and reaction pathways for the SAC of acetone over a TiO_2 catalyst at 300 °C, 350 °C and 400 °C.

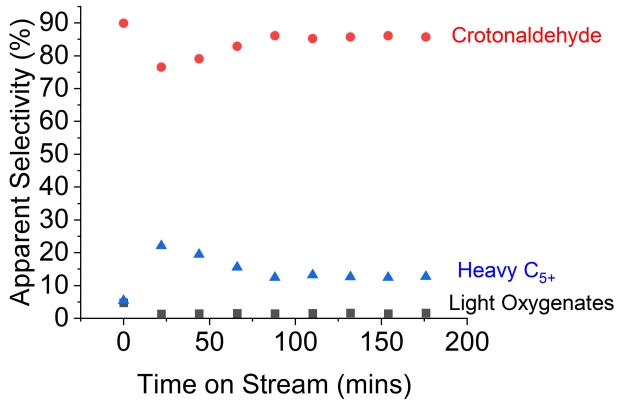

Supplemental Figure 4. TOS selectivity for low temperature acetaldehyde SAC: Time on stream selectivity data for a pure feed acetaldehyde SAC reaction.

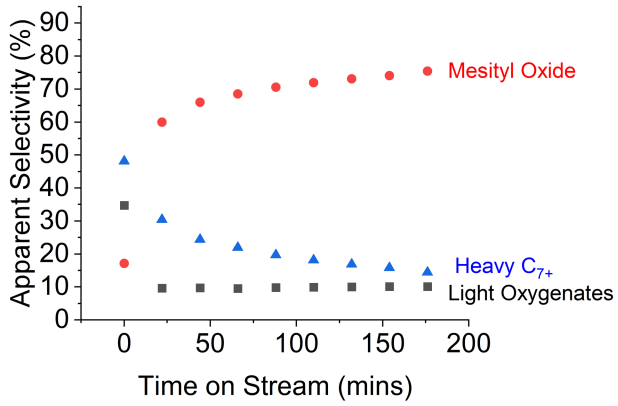

Supplemental Figure 5. TOS selectivity for low temperature acetone SAC: Time on stream selectivity data for a pure feed acetone SAC reaction.

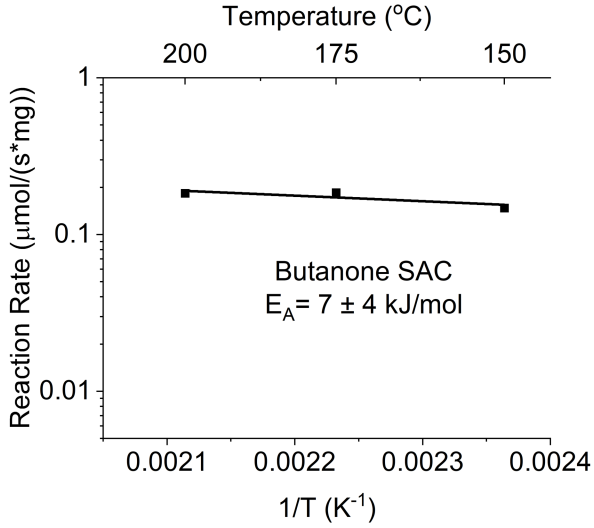

Supplemental Figure 6. Arrhenius plot SAC of butanone: Reaction rates calculated based on four unidentified primary products generated during the reaction. The activation barrier was calculated to be 7 ± 4 kJ/mol.

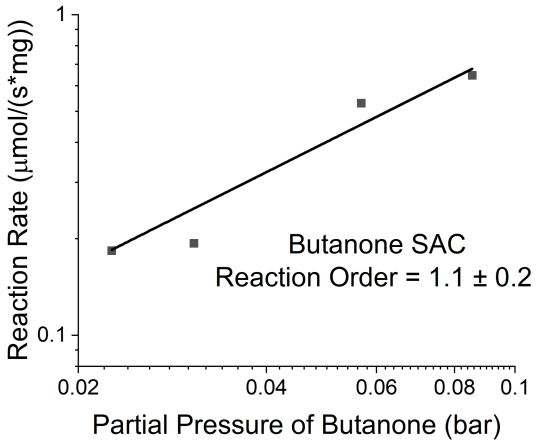

Supplemental Figure 7. Reaction order plot SAC of butanone: Reaction order plot for butanone SAC. Reaction rates calculated based on four unidentified primary products generated during the reaction. The reaction order was calculated to be 1.1 ± 0.2.

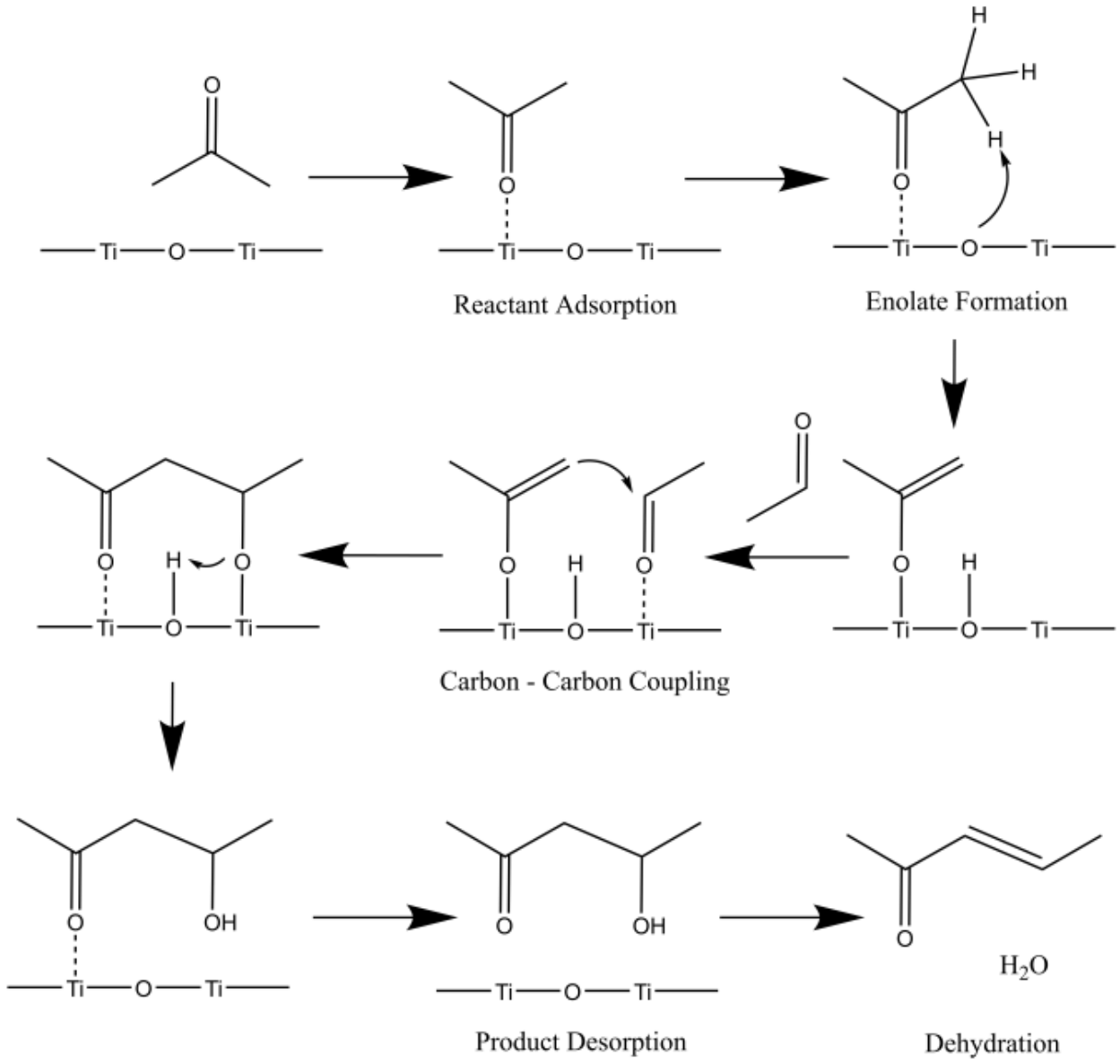

Supplemental Figure 8. Cross condensation reaction mechanism: Reaction mechanism for acetaldehyde and acetone cross condensation to produce 3-penten-2-one.

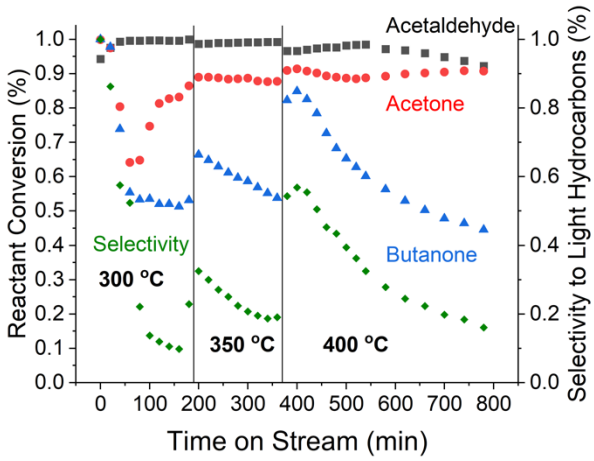

Supplemental Figure 9. TOS conversion for equimolar ternary MAC: Time on stream conversion data for equimolar ternary aldol condensation reactions at 300 °C, 350 °C and 400 °C. Selectivity to light hydrocarbon products (<C_5) is also shown.

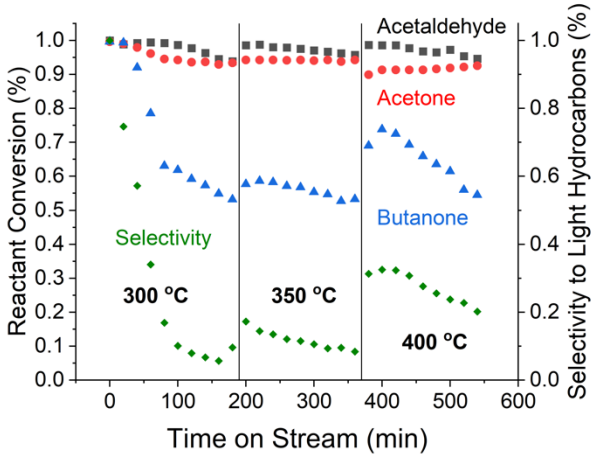

Supplemental Figure 10. TOS conversion for commercial molar ratio ternary MAC: Time on stream conversion data for 5.7:4.7:1 molar ratio of acetaldehyde, acetone and butanone ternary aldol condensation reactions at 300 °C, 350 °C and 400 °C. Selectivity to light hydrocarbon products (<C_5) is also shown.

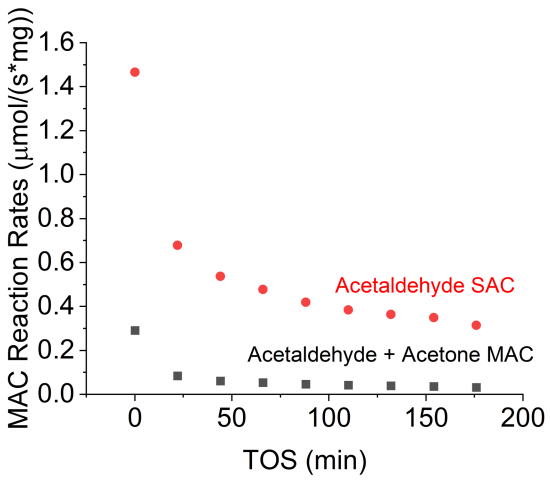

Supplemental Figure 11. TOS reaction rates for acetaldehyde and acetone MAC: Time on stream reaction rate data for an acetaldehyde and acetone MAC reaction at 200 °C.

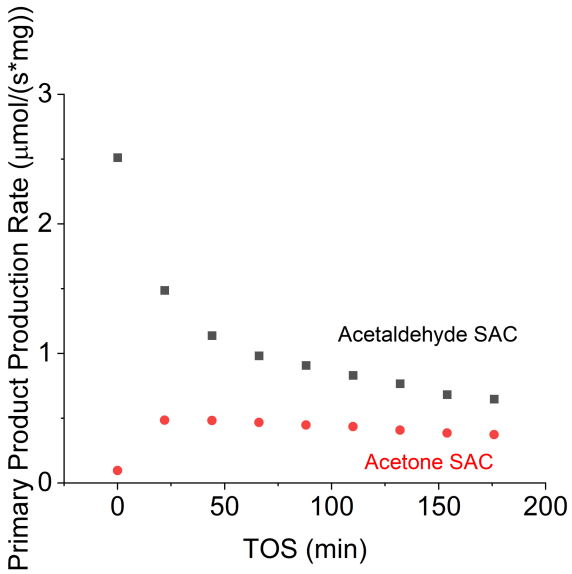

Supplemental Figure 12. TOS reaction rates for acetaldehyde and acetone SAC: Time on stream reaction rate data for pure feed SAC reactions at 200 °C.

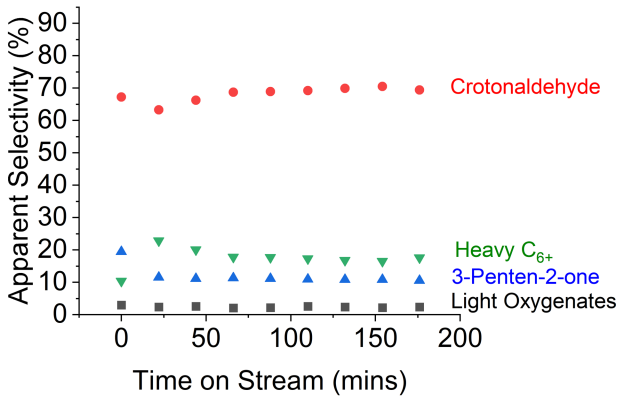

Supplemental Figure 13. TOS selectivity for acetaldehyde and acetone MAC: Time on stream selectivity data for an acetaldehyde and acetone MAC reaction.

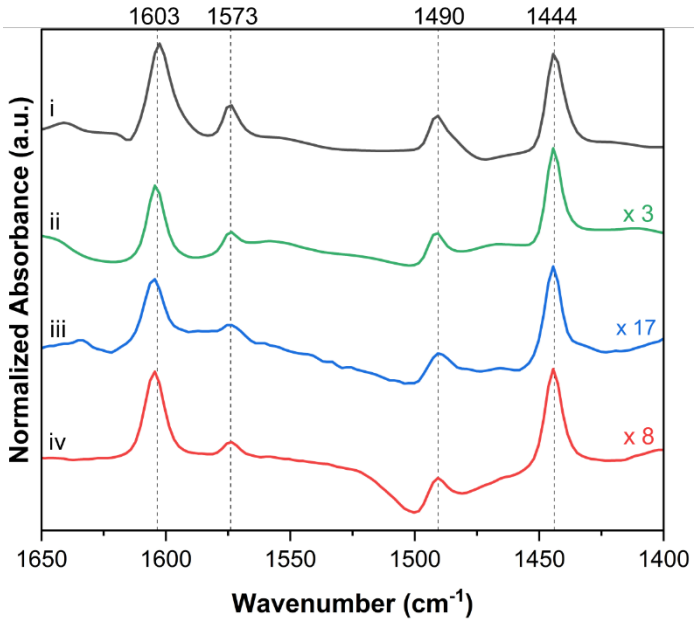

Supplemental Figure 14. Normalized DRIFTS spectra for pyridine chemisorption on TiO_2: DRIFTS Spectra for i. fresh TiO_2, ii. TiO_2 after adsorption of acetone, iii. TiO_2 after adsorption of acetaldehyde and iv. spent TiO_2. Spectra are normalized such that the peak at 1444 cm^{-1} has the same height. Normalization factors, calculated from averaging duplicate experiments, are ii. 2.7 ± 0.7, iii. 16.6 ± 1.2, and iv. 7.9 ± 0.6

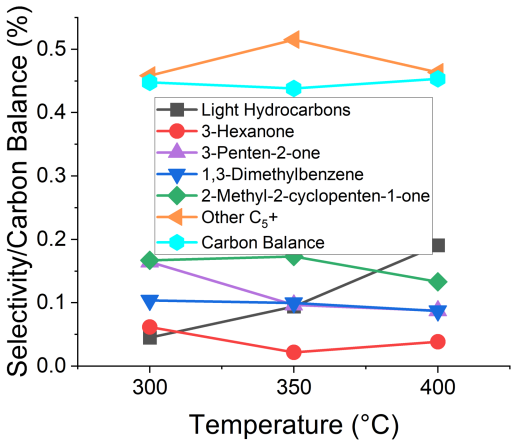

Supplemental Figure 15. Selectivities and carbon balances for ternary mixtures of acetaldehyde, acetone and butanone fed in molar ratios of 5.7:4.7:1: Molar ratios are for acetaldehyde, acetone and butanone respectively.

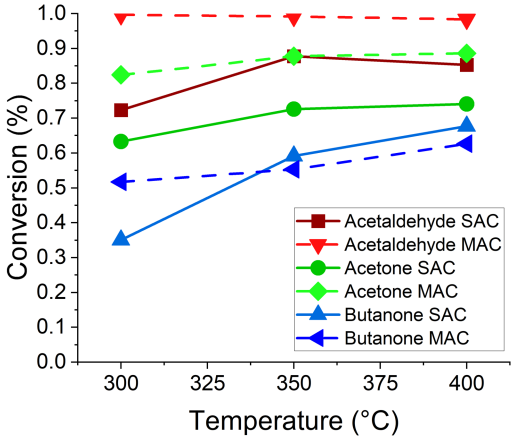

Supplemental Figure 16. Conversion for an equimolar, ternary mixture of acetaldehyde, acetone and butanone: Conversions of each component in the ternary mixture (dotted lines) are plotted alongside pure-feed SAC reaction conversions (solid lines).

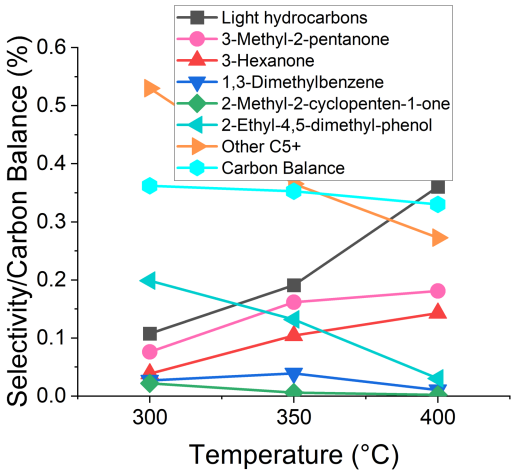

Supplemental Figure 17. Selectivities and carbon balances for ternary mixtures of acetaldehyde, acetone and butanone fed in equimolar molar ratios.

Supplemental Discussion of Figures S16 and S17: An equimolar mixture of all three components was investigated for direct comparison to the pure-feed and binary mixture studies. The conversion and selectivity are plotted as a function of reaction temperature in Figures S16 and S17. Surprisingly, for the equimolar ternary reaction (Figure S16), conversion of acetaldehyde and acetone was enhanced compared to the SAC reactions while the conversion of butanone remained relatively unchanged. The product mixture contained a wide range of low-yield reaction products (Figure S17), recorded as other C_{5+} products. This diverse product stream is likely due to the increased complexity of the reactant mixture and the wider range of possible condensation pathways. One of the primary reaction products observed at all temperatures from the equimolar reaction mixture is the acetaldehyde/butanone cross-condensation product 3-methyl-2-pentanone. The only identified product that was also observed in a SAC reaction was 2-methyl-2-cyclopenten-1-one, which is generated from acetaldehyde self-condensation.

Carbon balances for these reactions were poor, as shown in Figure S15 and Figure S17. This is likely a reflection of the GC only capturing vapor phase reaction products. A significant fraction of heavy, nonvolatile reaction products was found to condense in the lines between the reactor and the GC. These products were not accounted for in the selectivity or carbon balance analysis. Additionally, carbon deposition on the catalyst surface may have contributed to the carbon balance being lower than expected.

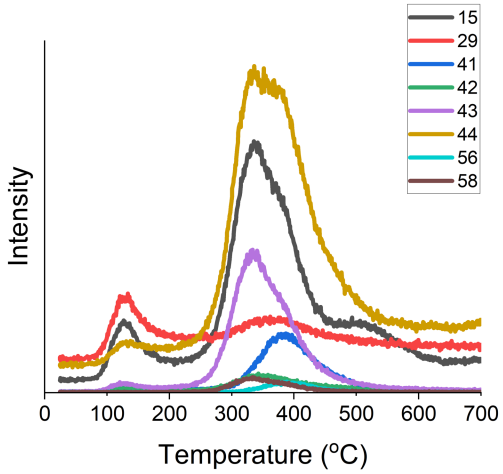

Supplemental Figure 18. Acetaldehyde TPD with additional mass fragments: Evolution of larger mass fragments during the acetaldehyde TPD shows the desorption of coupling products in the 300-500°C range.

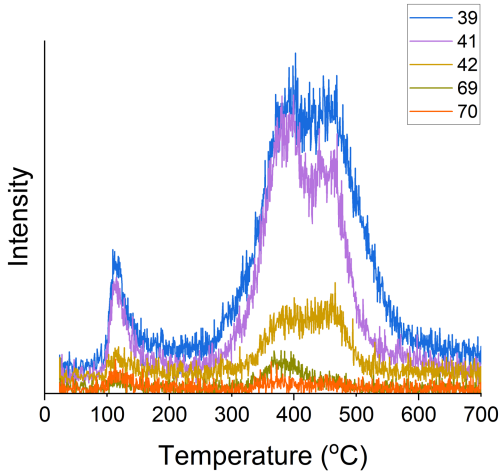

Supplemental Figure 19. Crotonaldehyde TPD with additional mass fragments: Crotonaldehyde TPD shows multiple desorbing products as indicated by high-temperature peaks with different fragmentation patterns, similar to what was observed during the acetaldehyde TPD.

Supplemental Table 1. Identified C_{5+} products from ternary MAC reactions

Molecule	Molecular Formula
Phenol, 2-ethyl-4,5-dimethyl	$C_{10}H_{14}O$
Phenol, 2-ethyl-4,5-dimethyl	$C_{10}H_{14}O$
Phenol, 2-ethyl-4,5-dimethyl	$C_{10}H_{14}O$
Phenol, 2-ethyl-4,5-dimethyl	$C_{10}H_{14}O$
Phenol, 2,3,4,6-tetramethyl-	$C_{10}H_{14}O$
2-5-Diethylphenol	$C_{10}H_{14}O$
(R)-3-Methyl-5-propylcyclohex-2-enone	$C_{10}H_{16}O$
Phenol, 2-(1,1-dimethylethyl)-3-methyl-	$C_{11}H_{16}O$
2,3,4,5,6-Pentamethylphenol	$C_{11}H_{16}O$
2,3,4,5,6-Pentamethylphenol	$C_{11}H_{16}O$
2,3,4,5,6-Pentamethylphenol	$C_{11}H_{16}O$
2,3,4,5,6-Pentamethylphenol	$C_{11}H_{16}O$
4-tert-Butyl-2,6-dimethylphenol	$C_{12}H_{18}O$
2,3,4,5,6-Pentamethylphenol, methyl ether	$C_{12}H_{18}O$
5-Methyl-2,4-diisopropylphenol	$C_{13}H_{20}O$
Phenol, 2,4-dimethyl-	$C_8H_{10}O$
Phenol, 3,4-dimethyl-	$C_8H_{10}O$
Phenol, 2,3-dimethyl-	$C_8H_{10}O$
2-Cyclopenten-1-one, 2,3,4-trimethyl-	$C_8H_{12}O$
Phenol, 2,3,5-trimethyl-	$C_9H_{12}O$
Phenol, 2-ethyl-5-methyl-	$C_9H_{12}O$
Phenol, 3,4,5-trimethyl-	$C_9H_{12}O$
Phenol, 2-ethyl-4-methyl-	$C_9H_{12}O$
Phenol, 2,3,5-trimethyl-	$C_9H_{12}O$
1-Cyclohexene-1-carboxaldehyde, 5,5-dimethyl-3-oxo-	$C_9H_{12}O_2$
2-Hydroxy-4,4,6-trimethylcyclohexa-2,5-dienone	$C_9H_{12}O_2$

C_{5+} products from the ternary mixed aldol condensation reaction (5.7:4.7:1 molar feed ratio for acetaldehyde, acetone and butanone respectively). Condensable components of the vapor phase product stream were collected by flowing the product stream into a chilled bubbler filled with acetone. The product-enriched acetone was then processed in an offline GC-MS for product identification.

Evaluation of Mass Transfer Effects

To determine the effect of internal mas transfer effects, the Weisz-Prater parameter was calculated using the following equation:

$$C_{WP} = \frac{-r'_A(obs)\rho_c R^2}{D_e C_{As}}$$

where C_{WP} is the Weisz-Prater parameter, $-r'_A(obs)$ is the observed production rate of the product with the highest selectivity, ρ_c is the pellet density, R is the pellet radius, D_e is the effective diffusivity and C_{As} is the reactant concentration at the catalyst surface. The effective diffusivity (D_e) was calculated using the following equation:

$$D_e = \frac{D_{AB}\varphi_p\sigma_c}{\tilde{\tau}}$$

where D_{AB} is the Knudsen diffusivity, φ_p is the pellet porosity, $\sigma_c$is the catalyst constriction factor and $\tilde{\tau}$ is the catalyst tortuosity. The Knudsen diffusivity (D_{AB}) was calculated using the following equation:

$$D_{AB} = \frac{d_{pore}}{3}\sqrt{\frac{8RT}{\pi M}}$$

Where d_{pore} is the catalyst pore diameter, R is the gas constant, T is the temperature, and M is the molecular weight of the reactant.

Using these three equations and the average values for tortuosity (3.0) and constriction factor (0.8) and the van der Waals equation of state to determine the reactant concentration at the catalyst surface, as well as the bulk density of the Aerolyst TiO_2 as the pellet density, the Weisz-Prater parameter was calculated to be $1.4*10^{-4}$ for the observed production rate of 0.27 μmol/(s-mg). Since this value is much less than unity, we can rule out internal mass transfer limitations for this system.

As another check that mass transfer limitations were negligible, we evaluated catalysts that were sieved to different particle sizes. Production rates for crotonaldehyde and 3-penten-2-one under mixed acetaldehyde / acetone condensation conditions were measured for TiO_2 with particle sizes of approximately 300 microns and approximately 70 microns. The production rate for crotonaldehyde was measured to be 11% higher for the larger particle size catalyst, while the production rate for 3-penten-2-one was measured to be 6% higher for the larger particle size catalyst. Such similar reaction rates over the wide range of catalyst particle size rules out major transport limitations.